Available online at www.sciencedirect.com
SciVerse ScienceDirect
Procedia Engineering 15 (2011) 554 – 560
Procedia Engineering
www.elsevier.com/locate/procedia

Advanced in Control Engineeringand Information Science

Research on Pointing Control Systems with Friction

Tang Puhua[a],Lei Yuyong[a*],Song Changlin[a],a*

[a]*School of Mechanical Engineering and Automation,Xihua University,Chengdu and 610039,China*

Abstract

Friction is inherent in mechanisms. In this paper a controller consisting of three schemes, proportional gain, pulse, and ramp (PPR), is proposed to achieve precise and fast pointing control under the presence of friction. Design of the PPR controller is based on two distinctive features of friction, the varying sticking force and presliding displacement of contacts. The latter is the main idea behind the ramp scheme to replace integration control, which induces slow dynamics in the sticking state. Simulation results demonstrate the robustness and effectiveness of the proposed controller.

Selection and/or peer-review under responsibility of [CEIS 2011]
Keywords: friction; PID; pointing systems;pointing control systems;

1. Introduction

Coulomb friction inherent in mechanisms poses a severe challenge to servomotor-controlled pointing systems. Many methods have been proposed to reduce the influence of friction on control systems, and these methods can be mainly divided into the model-based and the non-model-based approaches. The model-based methods try to estimate the friction load and counteract it by the opposite control [1, 2, 3, 4]. Some advanced approaches, such as robust schemes[5], nonlinear identification and feedback[6], and accelerated evolutionary programming[7] have been reported. But it has been pointed out that identifying this mode in the low-velocity regime is a difficult task[8]. To accomplish the identification requires a very

* Corresponding author. Tel.: +086-028-8772-9081; fax: +086-028-8772-9081.
E-mail address: yuyong_lei@mail.xhu.edu.cn.

1877-7058
doi:10.1016/j.proeng.2011.08.105

stiff low-velocity-control loop [1, 9]. Although the task is not easy, the model-based approach argues its value by removing the need for high-gain PI or PID controllers.

In contrast, the non-model-based approach applies various strategies to reduce the influence of friction without requiring its precise model. PI or PID types of controllers have been employed in industry for years because of their simplicity and robustness. In some systems, however, integral control suffers the hunting problem [10,11] and derivative control has to handle the noise in measurement. Using dither signals is a very popular, almost standard, technique for hydraulic servo actuators to reduce the impact of friction, but it is not recommended for electromechanical systems. As an alternative, impulsive control can reduce the sensitivity of the system to friction [1]. This scheme applies pulses to create a small displacement or a controlled breakaway, leading to transition to another control schemes [9, 10, 5, 12]. However, except with an especially designed apparatus [13], it is not easy to precisely create the designed displacement [10, 5]. Dual mode control integrates two modes of control in a single mechanism: gross motion in the regular way (macro dynamics) and fine motion in the range of presliding displacement (micro dynamics) [14, 15, 16]. A typical problem with this control scheme is that intermediate motions, pointing distances that are outside the ranges of the macro and the micro dynamics, are difficult to accurately control [16].

In this paper, we propose a three-scheme controller, one proportional gain, one pulse, and one ramp (PPR), to achieve fast and precise pointing control for systems with friction. The pulse scheme is designed to break the possible stuck condition during reverse motion and thus shorten the transient period. The ramp scheme takes advantage of the elastic deformation of contacts under static friction to achieve μm-level pointing accuracy. The transition between schemes is determined simply by the error and the velocity of the system. Simulation results are presented to demonstrate the effectiveness of the proposed PPR controller. The rest of this chapter is arranged as follows. Section 2 introduces the design of the PPR controller and Section 3 provides experimental results. Section 4 concludes this paper.

2. Principle of the Proposed Controller

The PPR controller is composed of three schemes, and Fig.1 gives a block diagram of the system with the configuration of the controller illustrated. This controller uses the error (e) and the velocity ($\dot{y}$) to determine the transition between schemes. Although this may lead to some noise in $\dot{y}$ estimated, the estimation acts as a threshold only to determine the state of motion and the design of the PPR controller does not require very precise estimation of $\dot{y}$. It will be clear that the control laws of the PPR controller do not contain derivative terms.

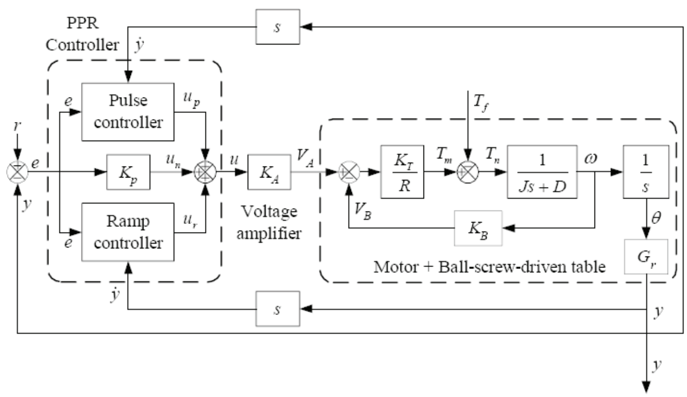

Fig. 1 Block diagram with the outline of the PPR controller.

With the estimation of $\dot{y}$, the idea behind the PPR controller is stated as follows. The P scheme drives the system toward the target. As the system gets closer to the target, it must slow down, then becoming liable to get stuck due to the increase of friction in the very low-velocity regime [1,17,18]. If the system stops moving, it will not restart until the control effort rises to an adequate level to overcome the maximum static friction force. This delay in the start of movement is usually not desirable for fast pointing control. Intuitively, the use of pulses can avoid such delays because they can break the possible adhesion caused by static friction. Thus, when the PPR controller estimates that the velocity is low and the error is still large, it switches to the pulse scheme to start the movement. As the error becomes so small that the pulse may cause the system to slide over the target, the ramp scheme is activated. This scheme achieves the precise positioning task by manipulating presliding displacement. Fig.2 illustrates how the e- $\dot{y}$ phase plane is divided into various regions for the three schemes.

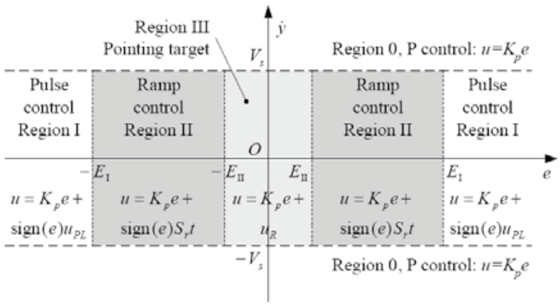

Fig.2 PPR control schemes in the *y*& - *e* phase plane.

Because static friction behaves in a very different way from dynamic friction does, it is important for the PPR controller to distinguish the state of motion. Here we define that the system is in motion if

$$|\dot{y}| > V_s \tag{1}$$

otherwise it is in the sticking mode. Ideally, V_s would be zero but practically it is not. Due to the strong dependence of *Vs* on the frictional mechanism and conditions of measurement, we propose to search for *Vs* from experiments. In this paper, we set V_s = 0.05 mm/s. As stated in above, taking the first difference on the position signal may lead to some noise, but the design of the PPR controller does not rely on very precise information of $\dot{y}$.

Region 0: The Proportional-Gain Scheme

From Fig. 2, Region 0 ($\dot{y} > V_s$) is the area in which the system is considered to be in motion. Since the influence of friction is not conspicuous unless the motion comes almost to a stop, it is not so necessary to compensate for Coulomb friction if the table is in motion. Therefore proportional-gain control is adopted in this region. Actually controllers of PD, PID, or any reasonable types can be candidates, but here the P controller is selected in order to demonstrate the simplicity and effectiveness of the proposed strategy. The control law in Region 0 is simply

$$u=K_pe \tag{2}$$

Region I: The Pulse Control Scheme

The design of the pulse scheme is based on two chief considerations. The first one is that the pulse shall be applied when the system stays in the sticking mode with an error larger than the designed tolerance E_{II}. On the other hand, it shall not be activated if the error is less than a critical value E_I (3 μm). The design of E_I is to prevent the system from limit cycling about the command position. These two considerations specify Region I in Fig.2,

$$|e| > E_I \ \ and \ \ |\dot{y}| \le V_s \tag{3}$$

The E_I in Eq.(3) is the error limit prohibiting the use of pulses. Determination of E_I requires the knowledge of presliding displacement. The control law in Region I is

$$u = K_p e + u_p = K_p e + u_{PL} sign(e) \tag{4}$$

Where u_{PL} is the pulse level. Although the design of a fixed u_{PL}(0.1 V)seems simple, choosing a proper level of u_{PL} still calls for deliberation to handle the uncertainties in practical situations.

Region II: The Ramp Control Scheme

The pulse scheme is not designed to complete the pointing task, but to drive the system to some locations close enough to the target so that the ramp scheme can proceed. The union of such locations is defined as Region II in Fig. 2,

$$|\dot{y}| \le V_s \ \ and \ \ E_{II} < |e| \le E_I \tag{5}$$

In this region, we propose the ramp scheme to achieve fast and precise pointing control. The control law is

$$u = K_p e + u_r = K_p e + sign(e)\int_0^t S_r d\tau \quad 0 < t \le T_r, S_r \ge 0 \tag{6}$$

where u_r is the ramp command, S_r is the slope of the ramp in Volt/sample, and t denotes time. T_r is the time specified for the ramp command to accomplish the pointing task. In this paper, the ramp slope S_r is designed to be a constant(S_r=1 mV/sample). Then u_r Eq. (6) can be represented by

$$u_r = sign(e) S_r t, 0 < t \le T_r, S_r \ge 0 \tag{7}$$

Here Eq. (7) is implemented by

$$u_r(k) = sign[e(k)] S_r + u_r(k-1) \tag{8}$$

The control law given in Eq. (6) is inspired by the microscopic movement, referred to as presliding displacement, between contacts under static friction.

Region III: The Target Region

The target region or Region III is defined by

$$|e| \le E_{II} \ \ and \ \ |\dot{y}| \le V_s \tag{9}$$

The control law in this region is

$$u = K_p e + u_r \tag{10}$$

where u_r is the ramp command at the sample when the system reaches Region III, a region bounded by E_{II} and V_s. Similar to the case of V_s, ideally E_{II} is zero but practically it is not. In this study, E_{II} is assigned according to the resolution of the position sensor (1μm), that is, E_{II}=0.5μm. This setting, however, does not imply that the positioning accuracy can be always equal to the limit of the resolution of the sensor. In practice, factors like measurement noise, performance of the power amplifier, and experiment conditions should be considered. Similar to the case in sliding mode control, a tight target region for the PPR controller is likely to induce chattering around the reference position.

The design of the PPR controller is introduced above. In summary, two parameters of friction, the ranges of presliding displacement, from which E_{II} is determined, and the static friction torque, which specifies the pulse level u_{PL}, are essential to the design task.

3. Simulation Results

The proposed PPR controller is evaluated on the system introduced in Table 1. Since the undamped natural frequency of the P-controlled system is lower than 10 Hz, the sampling rate F_s is set to be 250 Hz. Figure 3 depict the step responses of the system. In these tests, steps of different levels (0.05, 0.1, and 0.2 mm) were designed to investigate the influence of friction on the pointing performance. Responses and control efforts obtained by using PID, PI, and P controllers are also given in Fig.3 for comparison. With regard to the PID controller, we designed one for the linear system without friction but found that its performance is not satisfactory in experimental evaluations. The PI controller was obtained by removing the derivative term of the best-tuned PID controller.

Figures 4 and 5 present the pointing errors of the PID, PI, and PPR controllers. It is clear in Fig.5 that the PID controller fails to accomplish the pointing task. In contrast, the PPR controller demonstrates both fast and precise pointing performance, with most of the tasks accomplished within 0.5 seconds without overshoot, as shown in Fig.5.

A test for the robustness of the PPR controller is presented in Fig.6. In this test the table is loaded with a 20-kgw block and the PPR controller designed for the unloaded system is used. This load increases maximum static friction torque T_s and Coulomb friction torque T_c by about 12% and 5%, respectively. The damping coefficient D and the moment of inertia J are altered about 2% by this load. Although the change of D and J caused by this load is not much, the robustness of the PPR controller has been demonstrated through the distinct values of D, T_s, and T_c in both directions. The tolerance of the proposed controller for D is even larger. In addition to the satisfactory performance presented in Fig.6, one important feature of the ramp scheme is also noticeable.

Table 1 Parameters of the experimental system

Symbol and Name	Value
D, viscous damping	
(motor + load)	
Forward	50.46×10^{-3} N-m/rad/s
Backward	13.85×10^{-3} N-m/rad/s
G_r, gear ratio	$2/\pi$
J, moment of inertia	
(motor + load)	
Forward	2.02×10^{-3} N-m-sec^2
Backward	2.09×10^{-3} N-m-sec^2
K_A, gain of the voltage amplifier	19.88
K_B, back EMF constant	0.278 Volt/ rad/s
of the motor	
K_T, torque constant of the motor	0.278 N-m/ A
R, armature resistance	0.53 Ω

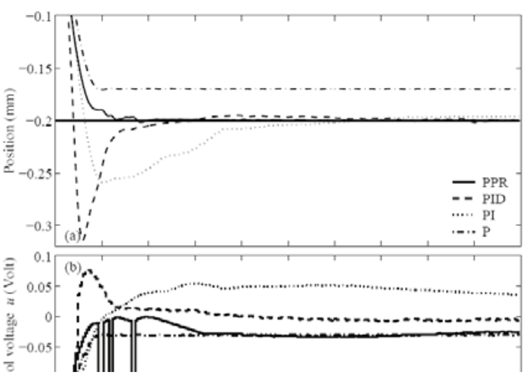

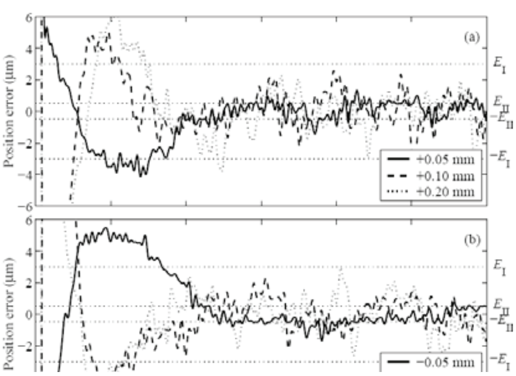

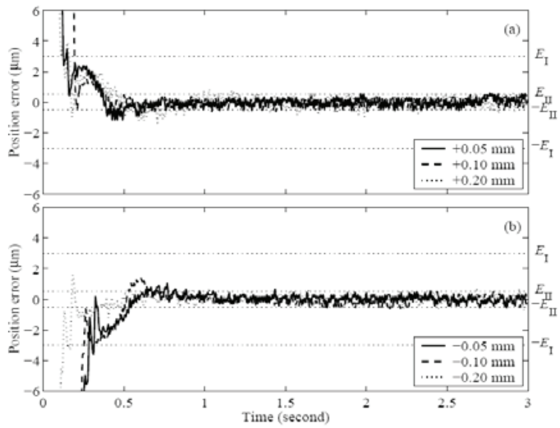

Fig.5 Pointing errors of the PPR controller.

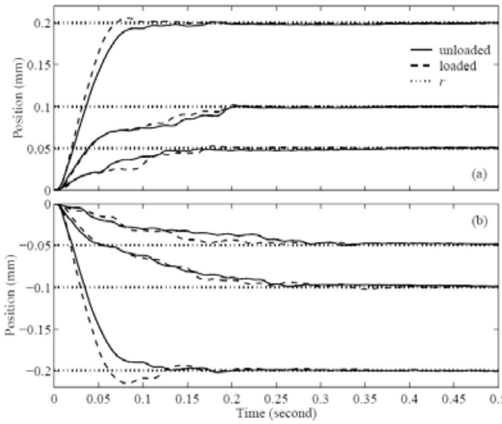

Fig.6 Robust test of the PPR controller.

4. Conclusions

In this paper, a controller consisting of proportional-gain, pulse, and ramp schemes has been proposed to accomplish precise and fast pointing control under the presence of friction. Each of the schemes, particularly the ramp scheme, was designed in accordance with the special features of friction in various regimes. We have analyzed the property of this particular scheme in eliminating the very tiny error caused by static friction and demonstrated its performance through simulation evaluations. In such evaluations, using the PPR controller could accomplish pointing tasks of various distances with up to 1-μm accuracy and without overshoot, whereas using the best-tuned PID controller inevitably suffered from 10% to 60% overshoots and took at least 2 times longer then the PPR controller to finish the task. Furthermore, although in different directions the experimental system were found to have at least 50% variation in the friction parameters, the PPR controller still demonstrated uniform performance in the two directions.

Acknowledgements

This work was financially supported by National Natural Science Foundation of China (50844033) and Key Research Lab Project of Sichuan Province Education Department (SZJJ2009-022).

References

[1] Armstrong-Hélouvry B, Dupont P, Canduas de Wit C. A Survey of Models, Analysis Tools and Compensation Methods for the Control of Machines with Friction. *Automatica* 1994;30:1083-1138.

[2] Swevers J, et al. An Integrated Friction Model Structure with Improved Presliding Behavior for Accurate Friction Compensation. *IEEE Trans. on Automatic Control* 2000;45: 675-686.

[3] Canudas de Wit, C., Noël, P., Aubin, A., and Brogliato, B., 1991, “Adaptive Friction Compensation in Robot Manipulators: Low Velocities,” *The Inter. J. of Robotics Research*, Vol. 10, No. 3, pp189-199.

[4] Canudas de Wit, C., Astrom, K. J., and Braun, K., 1987, “Adaptive Friction Compensation in DC-Motor Drives,” *IEEE J. of Robotics and Automation*, RA-3, No. 6, pp681-685.

[5] Southward SC, Radcliffe CJ,MacCluer CR. Robust Nonlinear Stick-Slip Friction Compensation. *ASME J. of Dynamic Systems, Measurement and Control* 1991;113:639-645.

[6] Johnson CT,Lorenz RD. Experimental Identification of Friction and Its Compensation in Precise, Position Controlled Mechanisms. *IEEE Trans. on Industry Applications* 1992;28:1392-1398.

[7] Kim JH, et al. Identification and Control of Systems with Friction Using Accelerated Evolutionary Programming. *IEEE Trans. on Control Systems* 1996;16:38-47.

[8] Canudas de Wit C,Lischinsky P.Adaptive Friction Compensation with Partially Known Dynamic Friction Model. *International Journal of Adaptive Control and Signal Processing* 1997; II:65-80.

[9] Armstrong-Hélouvry B.*Control of Machines with Friction*. Norwell, MA: Kluwer;1993.

[10] Yang S, Tomizuka M. Adaptive Pulse Width Control for Precise Pointing Under the Influence of Stiction and Coulomb Friction. *ASME J. of Dynamic Systems, Measurement and Control* 1988;110:221-227.

[11] Canudas de Wit C, et al. A New Model for Control of Systems with Friction. *IEEE Trans. on Automatic Control* 1995;40:419-425.

[12] De Weerth SP, et al. A simple neuron servo. *IEEE Trans. on Neural Networks* 1991;2:248-251.

[13] Hojjat Y,Higuchi T. Application of Electromagnetic Impulsive Force to Precise Positioning. *International Journal of Japan Society, Precision Engineering* 1991;25:39-44.

[14] Huang SJ, Yen JY, Lu SS. Dual Mode control of a System with Friction. *IEEE Trans. on Control Systems Technology* 1999;7:306-314.

[15] Futami S,Furutani A,Yoshida S.Nanometer Positioning and Its Micro-Dynamics. *Nanotechnology* 1990;1: 31-37.

[16] Ro PI,Hubbel PI. Model Reference Adaptive Control of Dual-Mode Micro/Macro Dynamics of Ball Screws for Nanometer Motion. *ASME J. of Dynamic Systems, Measurement and Control* 1993;115:103-108.

[17] Rooney GT,Deravi P.Coulomb Friction in Mechanism Sliding Joints. *Mechanism and Machine Theory* 1982;17:207-211.

[18] Wu R,Tung P. Studies of Stick-Slip Friction, Presliding Displacement and Hunting. *ASME J. of Dynamic Systems, Measurement and Control* 2002; 124:111-117.